Applied Food Research 6 (2026) 101967

Contents lists available at ScienceDirect

Applied Food Research

journal homepage: www.elsevier.com/locate/afres

Sample pretreatment and extraction method dictate the untargeted lipidomics profile of *Fucus vesiculosus* detected by ultra-high performance liquid chromatography-mass spectrometry

Cong Ding, Mikael Fabritius, Baoru Yang *

Food Sciences Unit, Department of Life Technologies, Faculty of Technology, University of Turku, FI-20014 Turku, Finland

ARTICLE INFO

Keywords:
Design of experiments
Extraction method
Fucus vesiculosus
Lipidomics
Sample pretreatment
Standardization

ABSTRACT

Untargeted food lipidomics is increasingly applied in food research. Yet the impact of pretreatment and lipid extraction methods on the lipidomics profiles detected in food matrices has not been systematically characterized. We used the brown macroalgae *Fucus vesiculosus* as a model to examine how these factors shape the lipid recovery and lipidomic profiles detected using ultra-high performance liquid chromatography-high resolution quadrupole time of flight mass spectrometry (RPLC–QTOF–MS/MS). Within Bligh & Dyer (BD) extraction system, homogenization time, ultrasonication time and extraction cycles significantly altered total lipid yield and the number of detected lipids. Homogenization and ultrasonication as sample pretreatments improved recovery of glycolipids and phospholipids, whereas prolonged treatments led to the loss of highly unsaturated polar lipids. Increasing the water phase in the solvent system had little effect on lipid yield but reduced the number of polar lipid species detected. Under identical pretreatments, BD and Folch extractions yielded similar total numbers of lipid species (~270) but clearly different class distributions: Folch extraction favoured TG and SQDG, whereas BD extraction enriched MGDG and several betaine-type lipids. These results show that both pretreatment conditions and choice of extraction methods can markedly influence lipid yields, polar lipid coverage, and relative abundance of different lipid classes. Careful design and transparent reporting of extraction protocols are therefore essential for robust and comparable food lipidomics.

1. Introduction

Lipidomics is an important part of metabolomics that focuses on comprehensive analysis of all lipid molecules in biological systems (Lam et al., 2017). In food research, untargeted lipidomics is increasingly employed to gain a full view of complex lipid profiles without predefined targets (Sun et al., 2020). It can be applied to study nutritional value and bioactive compounds, to assess quality and authenticity, and to monitor changes in lipids during processing and storage (Han & Gross, 2022), where comprehensive and unbiased lipid coverage is crucial.

However, untargeted lipidomic outcomes are highly dependent on the sample preparation method, especially the initial lipid extraction step (Rakusanova & Cajka, 2024). Lipids differ significantly in their structures and properties, such as polarity and solubility. Different solvents often show selectivity and differ in efficiency in extracting various lipid classes, including triglycerides (TGs), phospholipids (PLs), glycolipids (GLs), and sphingolipids (SLs) (Saini et al., 2021a). Therefore, a systematic evaluation is needed to determine how commonly used pretreatment and extraction strategies affect untargeted lipidome coverage and the relative abundance of lipid classes, rather than optimizing a single extraction condition. Moreover, the food matrix adds another layer of complexity. For example, modified Folch protocols are commonly used for milk (Li et al., 2017) and fish samples (Cao et al., 2024). Conversely, the Bligh & Dyer (BD) method is often used for microalgae and macroalgae (Conde et al., 2024). Over the years, many variations have been introduced on top of these original methods (Bligh & Dyer, 1959), including changes in solvent ratios, solvent-to-solid ratio, and number of extraction cycles (Figueiredo et al., 2019). Therefore, selecting an appropriate extraction method for each matrix is essential and remains a key challenge for standardizing food lipidomics. As a result, extraction protocols have become a major source of variability in lipidomics data (Kumari et al., 2011). Differences in pretreatment and extraction methods often result in variation in the

* Correspondence author.
E-mail address: baoru.yang@utu.fi (B. Yang).

https://doi.org/10.1016/j.afres.2026.101967
Received 2 January 2026; Received in revised form 9 March 2026; Accepted 3 April 2026
Available online 4 April 2026

lipidomics profiles and make it difficult to compare results between laboratories or studies.

Macroalgae are a good case study for this problem. They are rich in essential omega-3 (n-3) and omega-6 (n-6) polyunsaturated fatty acids (PUFAs) and contain diverse GLs, PLs and betaine lipids (BLs) with potential health benefits (Karageorgou et al., 2023). Wang et al. (2022) used LC-MS/MS to characterise the lipidomes of *Laminaria japonica, Undaria pinnatifida*, and *Sargassum natans* using BD-based extraction protocols. Notably, Gao et al. (2018) used the Folch method to extract lipids from the same species, *Laminaria japonica,* resulting in a different lipid profile. This makes their results difficult to compare with those of Wang et al. (2022). The reported lipid profiles of *Fucus vesiculosus* vary across studies. For example, Da Costa et al. (2019) applied the BD extraction and focused on the polar lipids, identifying 187 molecular species across 18 polar lipid classes. In contrast, Pham et al. (2024) used a methyl tert-butyl ether (MTBE) extraction procedure to profile both neutral and polar lipids, reporting that neutral lipids (TG/DG) accounted for 72–82 % of total lipids. Therefore, methodological heterogeneity may be mistaken for biological variation and can also mask true differences associated with origin, harvest season, and processing. This issue has become more evident with untargeted lipidomics, which enables deeper coverage of seaweed lipidomes and reveals strong matrix-dependent lipidomic patterns (Gowda et al., 2022). In addition, photochemical derivatization workflows coupled to untargeted HRMS/MS have enabled double-bond localization in edible seaweed lipids (Montone et al., 2024), further highlighting that extraction and pretreatment can shape not only "how much" lipid is recovered but also "what types of lipid structures" are observed. Together, these advances underline the need for robust and well-reported sample pretreatment and extraction workflows to reduce protocol-driven bias.

At the practical level, algae have rigid cell walls, so efficient cell disruption is needed to enhance the lipid extraction. Common pretreatments include mechanical homogenization and ultrasonication. For example, Marques et al. (2023) used UHPLC–MS to compare the lipidomics profiles of *Ulva rigida* and *Chlorella vulgaris*, identifying 462 lipid species across GLs, PLs, and BLs. However, they used different extraction settings (solvent, time, temperature), which limits cross-study comparisons (Lopes et al., 2021). Differences in pretreatment conditions and solvent systems make cross-study comparison difficult and make it hard to separate biological variation from methodological bias. This highlights the need to systematically study how extraction methods and pretreatment parameters influence untargeted lipidomic profiles, rather than assuming that one protocol is universally suitable for all types of food matrices.Design of experiments (DoE) offers a structured way to investigate the effects of different factors e.g. temperature, extraction time, solvent ratios, and number of extraction cycles, on the yield of extraction and the profile of the lipid extract.(Heavisides et al., 2018; Bowden et al., 2019). This approach helps to identify the most important factors and their interactions. In natural product research and extraction optimisation, DoE is widely used because it can improve protocols while reducing the number of required experiments (Uhoraningoga et al., 2018). In food lipidomics, however, DoE remains seldom applied for systematically assessing pretreatment- and extraction-driven changes in lipid coverage.

In this work, the aim was to examine how pretreatment and extraction conditions influence untargeted lipidomic profiles using *F. vesiculosus* as a model matrix. First, we applied a 2^4 factorial design within the BD system to evaluate the effects of homogenization time, ultrasonication time, number of extraction cycles and solvent-to-solid ratio on total lipid yield. After this, we conducted single-factor test series around the factorial settings to further optimize the extraction conditions, using gravimetric total lipid yield as the primary optimization criterion, and then analyzed the extracts by RPLC–QTOF–MS/MS to assess lipid-class distribution and molecular-species coverage. Finally, we compared the BD protocol with the Folch protocol under identical pretreatment conditions. Instead of proposing a single optimal extraction method, the aim of this study was to demonstrate how classical liquid–liquid extraction systems and the settings of parameters applied in sample pretreatment and extraction can shape the lipidomics profiles of *F. vesiculosus* detected by subsequent LC-MS/MS analysis. The findings of this study further highlight the importance of matrix-specific standardization of protocols for sample pretreatment and extraction as well as transparent reporting in food lipidomics research.

2. Materials and methods

2.1. Sample collection and preparation

F. vesiculosus fronds were collected from Boskär (Parainen, Finland). After harvesting, about 150 g of fronds were rinsed with filtered seawater to remove epiphytes and debris, then frozen at −80 °C. The frozen samples were lyophilized in a vacuum freeze-dryer at −60 °C for 2–3 days. The dried fronds were stored at −80 °C until lipid extraction and analysis.

2.2. Chemicals and reagents

HPLC-grade methanol (MeOH) and chloroform ($CHCl_3$), used as lipid extraction solvents, were purchased from Sigma-Aldrich (St. Louis, MO, USA). LC–MS-grade acetonitrile (ACN) and isopropanol (IPA), employed in the mobile phase, were obtained from Fisher Scientific (Waltham, MA, USA). LC–MS-grade ammonium formate (purity ≥99.0 %), used as a mobile-phase additive, was obtained from Sigma-Aldrich (St. Louis, MO, USA). Ultrapure water was generated by a Millipore Milli-Q purification system (Millipore, Bedford, MA, USA).

2.3. Overall experimental design and rationale

We adopted a three-step comparative workflow to map relationships among sample-pretreatment parameters and to evaluate how extraction conditions shape lipidomic profiles (Fig. 1).

Step 1: Screening stage. A 2^4 factorial design (16 runs) with replicated center points was applied to the Bligh & Dyer (BD) system to test four factors: homogenization time, ultrasonication time, number of extraction cycles, and solvent-to-solid ratio. Total lipid yield (% w/w, dry weight) served as the primary response for simultaneous assessment of main effects and two-way interactions (**Table S1**) and was determined gravimetrically as described in Section 2.6. Replicated center points provided an internal estimate of pure error, and p-values for the factorial ANOVA were computed using the center-point pure error as the error term **(Table S1)**.

Step 2: Single-factor series. Based on the factorial results in Step 1 (the significant main effects and two-way interactions and the direction of their effects on lipid yield), we performed one-factor tests in the vicinity of the selected factorial condition by varying one parameter within a narrowed range while keeping the other factors constant. For each condition, three independent extractions ($n = 3$) were carried out from the same homogenized batch, and each extract was analyzed by RPLC–QTOF–MS/MS in both positive and negative ESI modes. Unless otherwise stated, summary values are reported as the mean across extraction replicates for each response, including total lipid yield and peak area.

Step 3: Method comparison. Finally, the BD protocol selected from step 2 was compared with the Folch protocol under identical sample-pretreatment settings. Replicate extraction and LC–MS/MS analysis were the same as in Step 2, with three independent extractions per condition ($n = 3$). The detailed description of the BD protocol is presented in Section 2.4, and that of Folch extraction in Section 2.5.

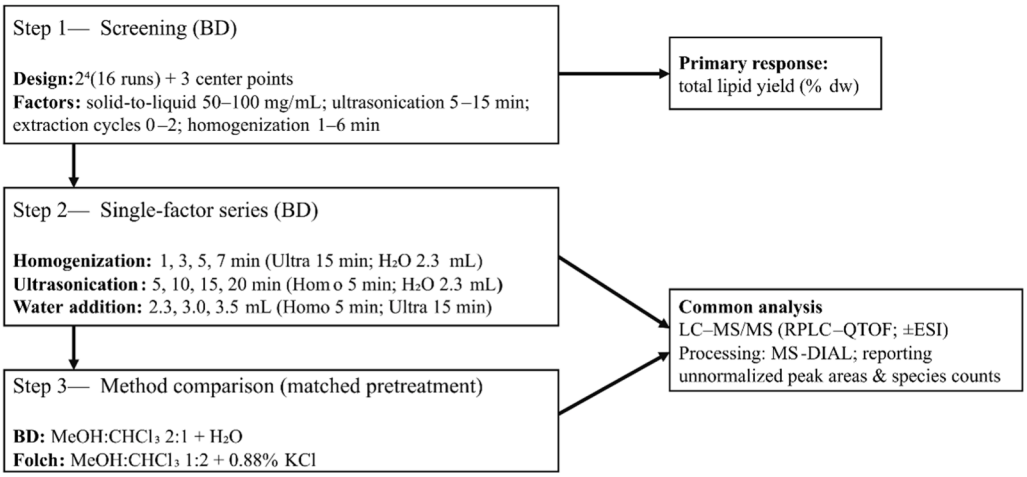

Fig. 1. Study design schematic. Three-step comparative workflow assessing internal standards were not used to allow direct comparison of raw signal intensities across conditions.

2.4. Optimised bligh & dyer (BD) method

For the modified BD extraction, 250 mg of the powdered *F. vesiculosus* sample was weighed into a 2 mL plastic vial and homogenized using a Tissuelyzer II bead mill (Qiagen, Germany) with 3 mm beads for 5 min (pausing after 2.5 min to reposition the sample and prevent overheating). The homogenized sample was transferred to a 15 mL centrifuge tube, and the original vial was rinsed with 3.75 mL of MeOH:$CHCl_3$ (2:1, v/v). After vortexing for 30 s, the mixture was sonicated in a Branson 5510 ultrasonic water bath (40 kHz) for 15 min, followed by centrifugation at 1460 g for 5 min. The supernatants containing all solvent phases were collected. The extraction was repeated two more times using 3 mL of MeOH:$CHCl_3$ (2:1, v/v), and all supernatants were combined and mixed with 2.3 mL of water. The sample was then centrifuged again at 1460 g for 10 min to separate the phases. The lower phase was transferred to a new container and dried under gentle nitrogen flow at 30 °C. The extract was weighed, redissolved in 1 mL of MeOH:$CHCl_3$ (2:1, v/v), and stored at −20 °C until analysis.

2.5. Folch method

For the modified Folch extraction, 250 mg of homogenized (5 min) *F. vesiculosus* powder was extracted using MeOH:$CHCl_3$ (1:2, v/v) as the solvent system. Initially, 3.75 mL of the solvent was added to the sample, followed by vortexing for 30 s and ultrasonication in a water bath for 15 min. The solvent was mixed with 2.3 mL of 0.88 % (w/v) KCl solution and then centrifuged at 1460 g for 5 min. The lower phase was transferred to a new container. This extraction procedure was repeated twice more using 3 mL of the same MeOH:$CHCl_3$ (1:2, v/v) each time. After combining all lower extracts, the lower phase was collected and evaporated under a gentle nitrogen flow at 30 °C. The dried extract was weighed and reconstituted in 1 mL of MeOH:$CHCl_3$ (1:2, v/v) prior to storage at −20 °C until analysis.

2.6. Gravimetric determination of lipid yield

After extraction, the dried extract was weighed to obtain the mass of the lipid extract. The lipid extract yield (%) was calculated based on the mass of extract using the following equation:

$$\text{Lipid Extract Yield } (\%, \text{dry weight}) = \frac{\text{Mass of lipid extract}}{\text{Mass of dried sample}} \times 100$$

2.7. Untargeted lipidomics analysis

2.7.1. RPLC–Q-TOF tandem mass spectrometry

Reverse-phase liquid chromatography (RPLC) was performed using an Elute HPG 1300 pump unit (Bruker Corp., Billerica, MA, USA) and an ACQUITY UPLC BEH C18 column (100 mm × 2.1 mm, 1.7 µm). Mass spectrometric analysis was carried out on an Impact II quadrupole time-of-flight tandem mass spectrometer (Bruker Corp., Billerica, MA, USA) with electrospray ionization (ESI) in both positive and negative modes. The samples were maintained at 10 °C in the autosampler, and the column oven temperature was set at 50 °C. Mobile phase A consisted of ACN/H_2O (60:40, v/v), and mobile phase B was IPA/ACN (90:10, v/v), each containing 10 mM ammonium formate. Mobile phase B was ultrasonicated in a water bath until all the ammonium formate dissolved. The injection volume was 1.0 µL in positive ion mode and 2.0 µL in negative ion mode. Lipid separation was achieved using a gradient of 40–100 % B over 0–18 min, 100 % B from 18 to 21 min, a return to 40 % B from 21 to 22 min, and re-equilibration at 40 % B until 25 min with a flow rate of 0.3 mL/min.

The nebuliser gas pressure was set at 2 bar, the drying gas flow rate at 8 L/min, and the drying gas temperature was at 300 °C. In positive ion mode, the capillary voltage was 5000 V, while in negative ion mode it was −3500 V. Full-scan mass spectra were acquired over an *m/z* range of 120–1200 in positive mode and 150–1200 in negative mode. MS/MS product ion spectra were obtained using data-dependent acquisition (DDA), targeting the top 10 ions per cycle with a spectra rate of 6 Hz. Collision energies were set to 35 eV in positive mode and 40 eV in negative mode.

2.7.2. Lipid annotation and peak-area integration

Raw LC–MS/MS files were processed with MS-DIAL v5.2 (Tsugawa et al., 2020). The parameters for feature detection are listed in **Table S2**. Preliminary lipid annotations were made using the LipidBlast library (Kind et al., 2013) and the built-in class-specific fragmentation rules for lipids in MS-DIAL. Each annotation was manually verified. We aimed to compare the influence of different extraction methods on the overall lipid profiles and the number of lipid species detected. Consequently, we did not include internal standards or calibration curves. Lipid peak areas were integrated using MS-DIAL v5.2 based on extracted ion chromatograms (EIC). All data processing parameters used in MS-DIAL, including peak detection, alignment, and identification settings, are detailed in **Table S3**. For data alignment, we did not process all files from all extraction conditions in a single global MS-DIAL project. Instead, for each extraction condition, the three replicate extracts were processed and aligned together within one MS-DIAL project, while identical peak

detection, alignment, and identification parameters were applied across conditions. A lipid species was considered present under a given extraction condition if it was detected in at least one of the three replicates after within-condition alignment. Cross-condition gap filling was not applied, because in this complex macroalgal matrix it increased the risk of integrating baseline noise as true signal and could artificially inflate Fill % and apparent lipid coverage. This strategy may underestimate the total number of lipid species recoverable across the full dataset, but it was considered more appropriate for a fair comparison of lipid species detected under different extraction conditions. Lipid profiles of the extracts were expressed as the percentages of peak areas of individual lipids of the total peak area sum of all lipid species detected, calculated using the following equation:

$$\text{Lipid peak area percentage } (\%) = \frac{\text{Peak area of an individual lipid}}{\text{Total peak area of all detected lipids}} \times 100$$

The peak areas used in the equation are MS1 precursor-ion EIC peak areas for each annotated lipid species without applying any class-specific response correction. Although this approach of lipidomics analysis does not provide the absolute quantity or relative abundance of individual lipids in the extracts, the data demonstrate shift in lipidomics profiles detected in response to changes in sample treatments and extraction methods.

2.8. Data analysis

Visualizations, including radar charts, bar graphs, and ring plots, were created using RStudio using the *fmsb* and *ggplot2* packages. In Step 1, the 2^4 factorial design was analyzed in Minitab (version 20, Minitab LLC, State College, PA, USA) to evaluate main effects and two-way interactions of pretreatment on gravimetric lipid yield, with replicated center points used to estimate pure error for ANOVA. In Step 2, differences among single-factor conditions ($n = 3$) were tested using one-way ANOVA in SPSS (version 30.0; IBM Corp., Armonk, NY, USA). Principal component analysis (PCA) was conducted in SIMCA 18 (Umetrics, Umeå, Sweden). Venn diagrams were generated via *jvenn* (Bardou et al., 2014) (https://jvenn.toulouse.inra.fr/app/index.html), and chord diagrams were produced in RAWGraphs 2.0 (https://app.rawgraphs.io/) after data processing.

3. Results and discussion

3.1. Effect of pretreatment settings on total lipid yield in the BD extraction

The DoE model (**Table S4**) showed significant main effects of homogenization time ($p < 0.001$), ultrasonication time ($p < 0.05$), and the number of extraction cycles ($p < 0.001$) on total lipid yield. These results indicate that even within the BD extraction method, small changes in sample pretreatment can lead to clear change in efficiency of lipid extraction. Homogenization breaks the rigid cell walls of *F. vesiculosus* and increases the access of solvent to cellular lipids. Extending homogenization therefore improved lipid yield **(Figure S1)**. Additional extraction cycles increased the frequency of solvent–solid contact, which also improved lipid yield. In contrast, ultrasonication mainly improved mass transfer between solvent and tissue. The dense cell wall of *F. vesiculosus* probably limited cavitation damage, so the effect of sonication time on yield was smaller than that of homogenization or extraction cycles **(Figure S1A)**, in line with previous reports (Carreira-Casais et al., 2021).

Interaction plots provided further insight into how these pretreatments work together (**Figure S1B**). The lines for ultrasonication and homogenization crossed, showing clear interaction between these two treatments i.e. the effect of ultrasonication depended on homogenization time. In contrast, the lines for ultrasonication and extraction cycles were nearly parallel, suggesting that the benefit of extra cycles was largely independent of sonication time. Within the BD workflow (Rey et al., 2019), water was added after organic solvent extraction to induce phase separation. When the total number of extraction cycles was set at two, varying the volume of water addition from2.3 to 3.5 mL- did not lead to notable change in total lipid yield (**Table S5C**). However, changing the water volume alters the solvent polarity and thus lipid species extracted. Therefore, we further performed untargeted lipidomic analysis to gain compositional insights beyond total yield.

3.2. Pretreatment settings change lipidomic coverage within the BD system

The lipid extracts obtained with different pretreatments followed by BD extraction using varying parameters were analysed using LC–ESI-MS/MS in both positive and negative mode. Under positive-ion mode, the lipids detected included mainly diacylglycerol (DG), triacylglycerol (TG), diacylglyceryl trimethylhomoserine and diacylglyceryl hydroxymethyl-N,N,N-trimethyl-β-alanine (DGTSA), lysodiacylglyceryl trimethylhomoserine and lysodiacylglyceryl hydroxymethyl-N,N,N-trimethyl-β-alanine (LDGTSA), as well as phosphatidylethanolamine (PE). All lipids were identified using MS-DIAL based on class-specific rule-based fragmentation patterns and matched against the LipidBlast database. Specifically, DGTSA and LDGTSA were determined based on the characteristic ion at *m/z* 236.149 (**Figure S2**), whereas PE was identified by neutral loss of 141.019 (**Table S2**) (Coniglio et al., 2021). We only kept features with a mass error below 5 ppm. All identified lipid species are presented **Table S6**. DGTSA showed the highest percentage of total peak area in the polar lipids (**Figure S3**) with 39 distinct species, while TG class showed the most diverse profile of neutral lipids, totaling 111 identified species. Phosphatidylcholine (PC) has been reported previously in *F. vesiculosus*. However, PC was not annotated in the present study. One plausible explanation is that zwitterionic betaine lipids such as DGTSA can partially substitute for PC in some algae, and the relative abundance of these classes may vary with environmental and growth conditions (Hoffmann & Shachar-Hill, 2023)

Venn analysis (Fig. 2**A and B**) showed how different treatments affected lipid coverage in BD extraction. When homogenization was extended to 7 min, more TG and PE species were detected, likely due to enhanced disruption of the cell walls of *F. vesiculosus*. At the same time, some DGTSA and LDGTSA species were not detected. A similar trade-off was seen for ultrasonication: longer ultrasonication released seven uniquely detected lipids but also led to the loss of some betaine-type lipids. This pattern may have been caused by heat production during mechanical treatment, which likely induced degradation of low-abundance polar lipids and promoted lipid oxidation during long pretreatment times (Du et al., 2023; Ganguly et al., 2024). As shown in Fig. 2**B**, increasing the ultrasonication time did not result in the detection of new PE, likely because PE remains closely associated with the cell wall, indicating that ultrasonication alone is not sufficient to release more PE from this macroalgae.

We also investigated the effect of water addition on the number of lipid species (Fig. 2**C**). Adding 2.3 mL water led to detection of two uniquely detected DGTSA and two uniquely detected PE species, suggesting that water volume can fine-tune the extraction of polar lipids. This effect may be attributed to the reduction in effective MeOH concentration, which increases the polarity of the upper MeOH/H_2O phase. If too much water is added, some of the polar lipids may remain dissolved in the upper phase instead of partitioning into the chloroform layer, leading to reduced overall recovery (Saini et al., 2021; Smedes & Askland, 1999). acyl carbon number:double bond range Although adding 3.5 mL water led to 9 uniquely detected TG species with similar acyl carbon number:double bond range (55–60:2–8) as those at 2.3 mL water (Fig. 2C), overall the tested range of water volumes had only a moderate impact on the lipid profile in positive ion mode. Negative-ion mode gave a complementary view on the impact of pretreatments and variables in BD extraction. Across all conditions, a total number of 101 lipid species

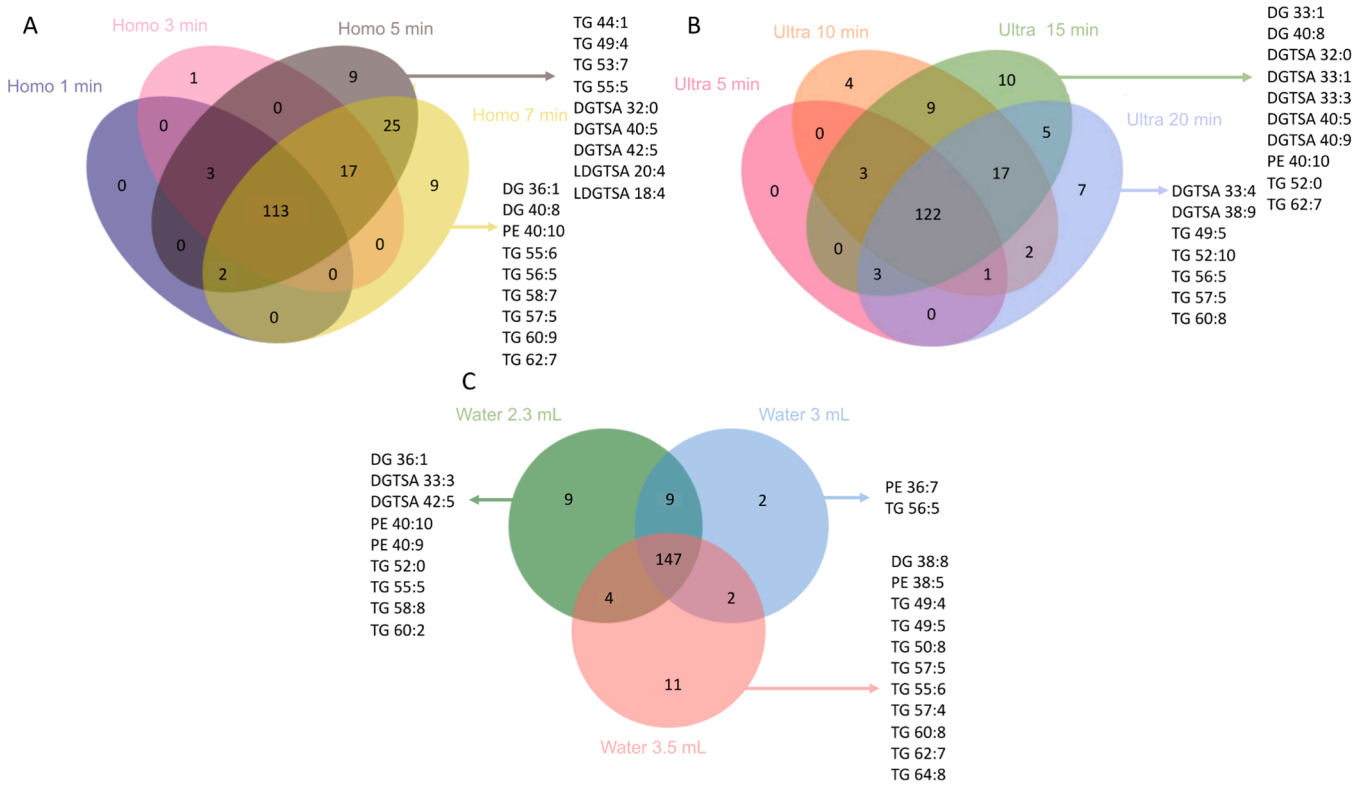

Fig. 2. Venn diagram of lipid molecular species identified in positive ionization mode in the different single-factor experiments. (A) Homogenization group, (B) Ultrasonication group, and (C) Volume of water group. Lipid classes: TG: triacylglycerol, DG: diacylglycerol, PE: phosphatidylethanolamine, DGTSA: diacyl-glyceryl-N,N,N-trimethylhomoserine/β-alanine, LDGTSA: lyso-DGTSA.

were identified (**Tables S6**). The radar plot (Fig. 3) shows that one BD setting (homogenization for 5 min, ultrasonication for 15 min, and 2.3 mL water added for phase separation) produced the broadest coverage, as indicated by the largest polygon area. However, prolonged pretreatment (long homogenization or long ultrasonication) clearly reduced the number of lipids detected, pointing to degradation under harsher conditions (Ganguly et al., 2024).

Among GLs, monogalactosyldiacylglycerol (MGDG), with 28 species detected identified (Fig. 3**A and B**) based on the headgroup ($C_6H_{17}O_8^-$; deprotonated galactosylglycerol) fragment ion at *m/z* 253.093 and the characteristic fatty acid fragments (**Figure S4**), contributed the highest proportion of total peak area in negative-ion mode (**Figure S3B**), MGDG in brown algae is rich in polyunsaturated fatty acids, which are susceptible to thermal and oxidative damage. It is therefore possible that extended homogenization lowers the number of detectable MGDG species. Digalactosyldiacylglycerol (DGDG) and sulfoquinovosyl diacylglycerol (SQDG) showed similar sensitivity, with fewer species detected when pretreatment was extended to 7 min for homogenization, and 20 min for ultrasonication. Interestingly, digalactosyl monoacylglycerol (DGMG) only appeared at the intermediate condition of 5-min homogenization and 15-min ultrasonication, further underlining how specific parameter combinations can either reveal or mask low-abundance glycolipids.

Among PLs, only one lysophosphatidylethanolamine (LPE) was detected in all samples, while multiple phosphatidylglycerol (PG) and phosphatidylinositol (PI) species were detected. PG was identified by its

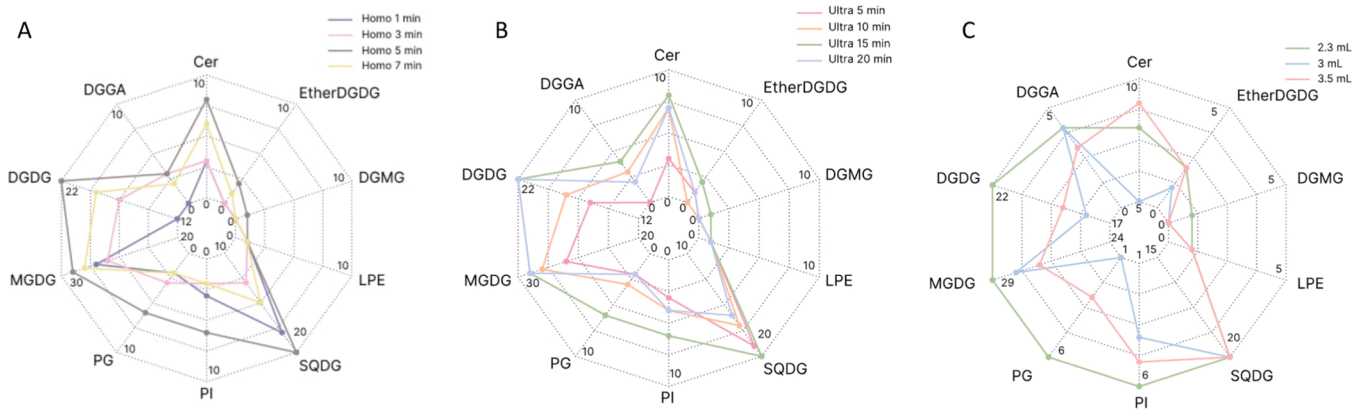

Fig. 3. Radar chart showing the number of different lipid classes detected in negative ion mode from single-factor experiments. (A) Homogenization experiment, (B) Ultrasonication experiment, and (C) Experiment on volume of water addition. Lipid classes: PE, phosphatidylethanolamine; LPE, lysophosphatidylethanolamine; PI, phosphatidylinositol; PG, phosphatidylglycerol; DGDG, digalactosyldiacylglycerol; SQDG, sulfoquinovosyldiacylglycerol; EtherDGDG, ether-linked DGDG; Cer, ceramide; DGMG, digalactosylmonoglyceride; MGDG, monogalactosyldiacylglycerol; DGGA, diacylglyceryl glucuronide.

headgroup at *m/z* 152.996 and PI was identified by its headgroup fragment at *m/z* 241.012, while the fatty acid fragments confirmed its molecular species composition (Kobayashi, 2016). With increasing homogenization and ultrasonication times, the number of PG species rose from two to six. A similar increase (to six species) was observed also for PI. Altogether, even low-abundance lipid classes, including minor glycolipids (DGMG and DGGA), were affected by the different pretreatment conditions. Finally, we also evaluated the effect of water volume on lipid detection in negative-ion mode. Taking MGDG (the class with the most species identified) as an example (Fig. 3**C**), the number of MGDG species decreased as volume of added water increased. This is likely because adding more water progressively alters the solvent polarity: some of the methanol in the chloroform layer is pulled into the aqueous phase, shifting the effective polarity of the organic layer (Ulmer et al., 2018). Interestingly, SQDG was less sensitive to solvent polarity changes, likely because the anionic headgroup kept the molecules in the organic phase (Shimojima, 2011). In contrast, the neutral galactolipids (MGDG and DGDG) contained highly polyunsaturated fatty acids. Thus, removing methanol from the chloroform layer lowers the organic phase's polarity (and solvent strength), reducing the solubility of those highly unsaturated lipids and decreasing the number of species extracted.

Overall, the results from both ion modes show that BD pretreatment settings reshape the lipidomic coverage. Longer homogenization and ultrasonication can increase the release of some lipids but may lead to the loss of specific low-abundance lipids. This effect was volume-dependent: within the tested range (2.3–3.5 mL), water volume had little impact on lipid yield (**Table S5C**), but progressively altered phase partitioning and reduced polar-lipid diversity (e.g., from 101 to 82 identified polar lipids in negative-ion mode at the highest water volume). Thus, even before changing the extraction solvent system, within the BD protocol it is possible to modify the coverage of lipid species by changing the pretreatments.

3.3. Comparison between BD and folch extraction methods: the different solvent systems shift the balance between neutral and polar lipids

Using the pretreatment settings optimized for the BD extraction, we compared BD and Folch extraction methods under identical sample-pretreatment conditions. The only difference was the solvent system. The two workflows differed in the organic solvent composition and in the aqueous phase used for phase separation (water in BD and 0.88 % KCl in Folch). Folch gave a slightly higher gravimetric yield (3.63 %) of total lipids than BD (3.44 %) (**Table S5D**), showing influence of the solvent system on lipid recovery from *F. vesiculosus*.

Despite the slight difference in total lipid yield, the extracts obtained with the two methods showed rather similar overall lipid class profiles in positive-ion mode, having TG and DGTSA as the dominating lipid classes, and DG, LDGTSA, and PE as the minor classes (Fig. 4**A**). Although TG and DGTSA remained as the dominant lipids in both extracts, the two extracts differed in the relative abundances of the two dominating classes: TG accounted for 69 % of total peak area in Folch extract compared to 62 % in BD extract, whereas the relative abundance of DGTSA (29 %) in the Folch extract was less than that (36 %) in BD. This suggests that the Folch solvent system with higher proportion of chloroform is more effective in extracting neutral lipids like TG (Figueiredo et al., 2019), while the BD system is more suitable for certain polar (betaine) lipids. Consistently, the Venn diagram (Fig. 4B) shows that the Folch method extracted additional neutral lipid species (including eight uniquely detected TGs) which were not found in the BD extract, the latter having four DGTSA and three LDGTSA species not present in the Folch extract.

In negative ion mode (Fig. 4**C**), MS-MS analysis detected clear differences in polar lipid profiles between Folch and BD extracts. MGDG was the most abundant lipid accounting for 48 % of total peak area in the BD extract, whereas SQDG dominated the Folch extract (49 %).

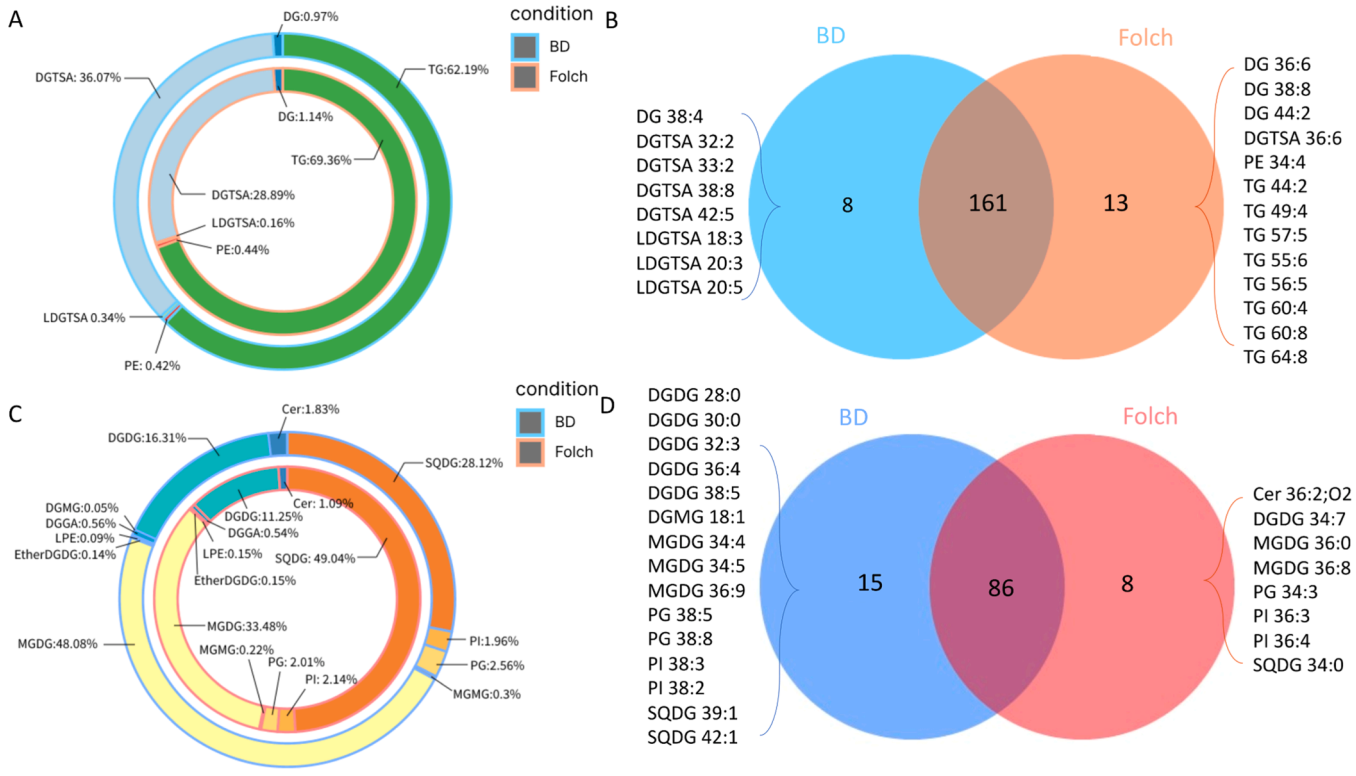

Fig. 4. Lipidomic profiles of *F. vesiculosus* extracted using the Folch and BD methods. (A) Peak area percentages of lipid classes detected in positive ion mode. (B) Lipid classes detected in positive ion mode (C) Peak area percentages of lipid classes detected in negative ion mode. (D) Lipid classes detected in negative ion mode Lipid classes: PE, phosphatidylethanolamine; PI, phosphatidylinositol; PG, phosphatidylglycerol; MGDG, monogalactosyldiacylglycerol; DGDG, digalactosyldiacylglycerol; SQDG, sulfoquinovosyldiacylglycerol; DGMG, digalactosylmonoglyceride; TG, triacylglycerol, DG, diacylglycerol; PE, phosphatidylethanolamine; DGTSA, diacyl-glyceryl-N, N, N-trimethylhomoserine/β-alanine; LDGTSA, lyso-DGTSA.

Compared to Folch extract, BD extract had higher number of polar lipid species including DGDG, MGDG, PG, and PI). In addition, the Folch extract also contained saturated MGDG species (36:0), whereas only unsaturated MGDG species (34:4, 34:5 and 36:9) were found in the BD extract (Fig. 4**D).** These together indicate that BD extraction favours polar lipid species compared to Folch extraction. The BD method identified 101 lipid species in negative mode, whereas only 98 species were detected in the Folch extract. The additional lipids extracted only by BD method generally had high degrees of unsaturation. The differences in SQDG and MGDG between methods likely stem from both solvent composition and matrix effects. The higher chloroform content in Folch's solvent favors non-polar or weakly polar lipids, and the sulfonate headgroup of SQDG is sufficiently hydrophobic to remain soluble in chloroform. Meanwhile, Folch may co-extract components (e.g., proteins or salts) that suppress the ionization of highly unsaturated MGDG (Iverson et al., 2001), making some of those species less detectable in the Folch extract. The 0.88 % KCl solution can facilitate phase separation and reduce emulsions, but differences in ionic strength may also influence phase partitioning and salt carryover, which can affect lipid recovery and LC–MS detectability.

Notably, certain low-abundance lipids such as diacylglyceryl glucuronide (DGGA) and an ether-linked digalactosyldiacylglycerol (EtherDGDG) were detected in both Folch and BD extracts. To our knowledge, this is the first report of DGGA and EtherDGDG in *F. vesiculosus*. **Figure S5A** shows the MS^2 spectrum of DGGA 14:0_18:1 ($[M–H]^-$ *m/z* 741.5147), with fragments confirming its fatty acid composition (*m/z* 227.2010, 281.2479) and a neutral loss (*m/z* 477.2740). DGGA was first discovered in microalgae, where these

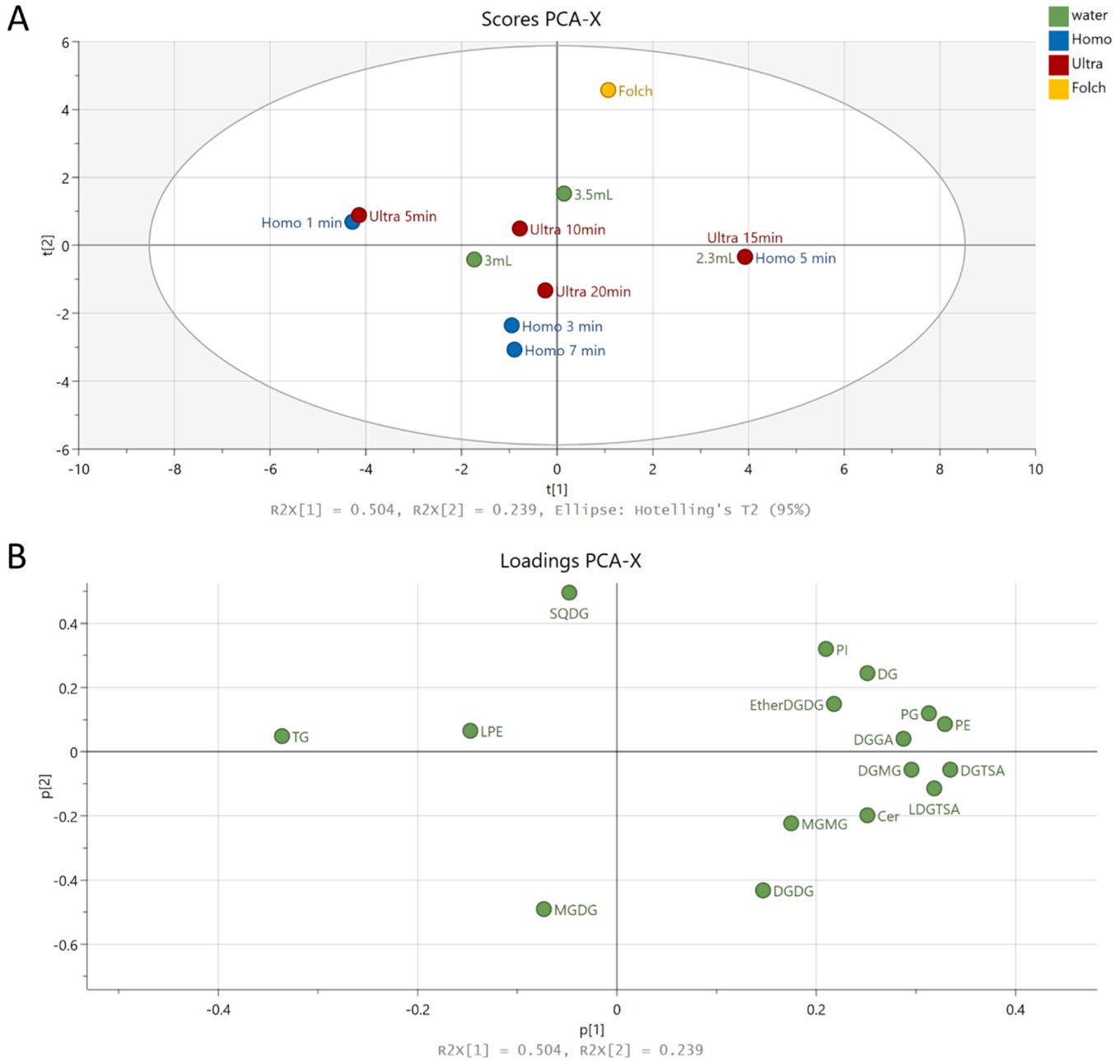

Fig. 5. Principal component analysis (PCA) score plot (A) and loading plot (B) constructed from peak area percentage of different lipid classes detected with different extraction methods. Lipid classes: LDGTSA, lyso-DGTSA; DGTSA, diacyl-glyceryl-N,N,N-trimethylhomoserine/β-alanine; PE, phosphatidylethanolamine; LPE, lyso-PE; PI, phosphatidylinositol; PG, phosphatidylglycerol; MGDG, monogalactosyldiacylglycerol; DGDG, digalactosyldiacylglycerol; SQDG, sulfoquinovosyldiacylglycerol; EtherDGDG, ether-Linked digalactosyldiacylglycerol; Cer, ceramides; DGMG, digalactosylmonoglyceride; MGMG, monogalactosylmonoglyceride; DGGA, diacylglyceryl glucuronide; Cer, ceramide; TG, triglycerides; DG, diglycerides.

compounds accumulate under phosphate starvation (Suzuki et al., 2025), indicating possible association of the lipidomic profile of *F. vesiculosus* with environmental growth conditions.

Similarly, EtherDGDG was also detected (**Figure S5B**) based on the $[M+HCOO]^-$ adduct ions (which is the same *m/z* as DGDG's adduct) and fragment ion at *m/z* 953.6325 resulting from loss of formate anion, which further underwent a neutral loss of C18:3 acyl chain producing a fragment at *m/z* 693.4406, and an additional fragment from further loss of H_2O. Due to the ether bond, only one free fatty acid fragment (C18:3 at *m/z* 277.2166) was seen the other fatty acyl chain remains bound. EtherDGDG has previously been reported only in green algae, where it may help stabilize photosynthetic membranes or modulate membrane fluidity under stress (Ishibashi et al., 2014).

Overall, the differences between BD and Folch were more pronounced in lipidomic profile detected in the negative-ion mode than in the positive-ion mode. BD extraction yielded a greater variety of polar lipids which are better detected in negative mode, whereas Folch tended to extract slightly more neutral lipids. Importantly, there was no significant difference between the two methods in the detection of very-low-abundance lipids like DGGA and EtherDGDG, indicating our pretreatment was sufficient for cell disruption in both cases. Although the total number of lipid species detected (270 lipid species by BD vs. 268 by Folch) were similar in extracts obtained with these two extraction methods, there were marked difference in peak area percentages of the major lipid classes. Taken together, these results suggest that pretreatment protocol governs the release of lipids from the tissues and cells, while the choice of solvent system strongly influences the relative abundance of lipid classes in the extract.

3.4. Multivariate analysis of extraction-dependent lipid profiles

Principal component analysis (PCA) was applied to demonstrate the impact of pretreatment within BD extraction and to show the difference between BD and Folch extraction using the same sample pretreatments. PCA was performed on the peak area percentages of lipid classes (Fig. 5). PC1 and PC2 explained 50.4 % and 23.9 % of the total variance, respectively, giving 74.3 % in total.

In the PCA score plot (Fig. 5**A**), the Folch extract located above all the BD-derived extracts on PC2. Among the BD samples, as homogenization and ultrasonication times increased, the lipid profile tended to shift toward higher scores of PC1 (more positive). However, extending homogenization from 5 to 7 min did not further increase the PC1 score, suggesting that stronger pretreatment does not necessarily extract more polar lipid. Increasing the water volume from 3.0 to 3.5 mL also shifted the BD sample scores towards the positive direction on both PC1 and PC2, making the BD lipid profile more closely resemble that of Folch.

The loading plot (Fig. 5**B**) clarifies the chemical basis of these separations. Polar lipids (e.g., PG, DGTSA) have strong positive loadings on PC1, whereas TG has a strong negative loading of PC1. Thus, PC1 essentially separates polar vs. neutral lipid dominance. It can be inferred that, under the BD protocol, changes in pretreatment mainly shift the lipid profile along this polarity axis (PC1). For example, samples with minimal homogenization (1 min) or ultrasonication (5 min) cluster toward the TG-rich, low-PC1 end, suggesting that easy-to-extract neutral lipids dominate when cell disruption is insufficient. More rigorous pretreatment is required to release polar lipids moving profiles toward the high-PC1 end. However, the non-monotonic behavior (e.g., the 7 min homogenization did not further increase PC1 score of the extract) suggests that excessive homogenization/sonication may generate heat or oxidation that degrades some lipids, to some extent counteracting the benefits of longer treatment time. PC2 appears to separate the extracts based on specific lipid classes. High abundance of SQDG contributed strongly to the positive PC2 direction, whereas high proportion of MGDG and DGDG drove the negative PC2 direction, demonstrating an inherent difference between Folch and BD extractions. Folch extraction enriched SQDG relative to MGDG, whereas BD did the opposite, which aligns with the earlier observation on favoring impact of Folch extraction on SQDG.

Fig. 6 provides an overview using a chord diagram linking 16 lipid classes to the 12 extraction conditions. In this diagram, longer arcs on the method side indicate a greater overall influence of that variable on lipid abundance. The conditions of 5 min homogenization, 15 min ultrasonication, and 2.3 mL water addition produced the longest arcs, suggesting that these factors (especially the pretreatment intensity) have the strongest impact on lipid yields and profiles. In contrast, changing water volume had a smaller effect on arc length than changing homogenization or sonication time. This implies that, although water volume can modify lipid partitioning, efficient cell disruption is more critical for extracting lipids from *F. vesiculosus*.

Each lipid class is colour-coded according to the condition that most strongly influenced it. The 2.3 mL water condition is linked to many classes, especially glycolipids and betaine lipids, highlighting its importance for these groups. Increasing water volume to 3.5 mL specifically enhanced the extraction of ceramides (Cer). With the exception of a few lipid classes (TG, DG, PI and PE), which were most strongly associated with the Folch extraction, most lipid classes were primarily linked to conditions within the BD extraction set. Taken together, the PCA and chord diagram support a two-level view of extraction effects. Pretreatment conditions mainly control how many lipid species are released from the macroalgal matrix, whereas the solvent system largely determines which classes are favored in the final lipidomic profile. This helps explain why lipidomic data from different studies can be difficult to compare when either or both pretreatment steps and extraction methods vary, highlighting the importance of matrix-specific optimization of lipid extraction protocols including sample pretreatments and extraction variables.

4. Conclusions

This study used a macroalgal species *Fucus vesiculosus* as a model food matrix to demonstrate the importance of sample pretreatment and extraction method variables in influencing the untargeted lipidomics profile detected in UHPLC-MS/MS analysis. Within the BD system, homogenization time, ultrasonication time and extraction cycles clearly influenced the total lipid yield and the number of lipid species detected. Appropriate pretreatment improved the yield of glycolipids and phospholipids, while very long treatments led to the loss of highly unsaturated polar lipids. Changing the volume of added water had little effect on yield but reduced polar-lipid diversity by altering phase partitioning.

Using the sample pretreatment conditions optimized for BD extraction, BD and Folch extractions produced extracts with similar total numbers of lipid species, however, differing in relative abundance of different lipid-classes. Folch favored TG and other neutral lipids, whereas BD extraction resulted in a higher proportion of polar lipids, including MGDG and betaine-type lipids. In negative-ion mode, BD enriched MGDG and related glycolipids, while Folch favored SQDG. Both extraction methods allowed the detection of minor lipids such as DGGA and EtherDGDG, indicating that, with sufficient cell disruption, structurally diverse and low-abundance lipids can be recovered in either solvent system.

Overall, our results show that both pretreatment settings and solvent choice are critical experimental variables in lipidomics analysis of food. Seemingly small changes in pretreatment such as homogenization, ultrasonication or in extraction variables such as water-phase composition can shift lipid yields, coverage of lipid species, and relative abundance of lipid classes. However, because no class-specific internal standards were applied, caution is needed when interpreting relative peak-area differences across lipid classes, as ionization efficiencies may vary between classes. The findings of this study highlight the importance of matrix-specific optimization of sample pretreatment and lipid extraction, as well as transparent reporting of are crucial to produce unbiased results, to interpret properly the findings and to make

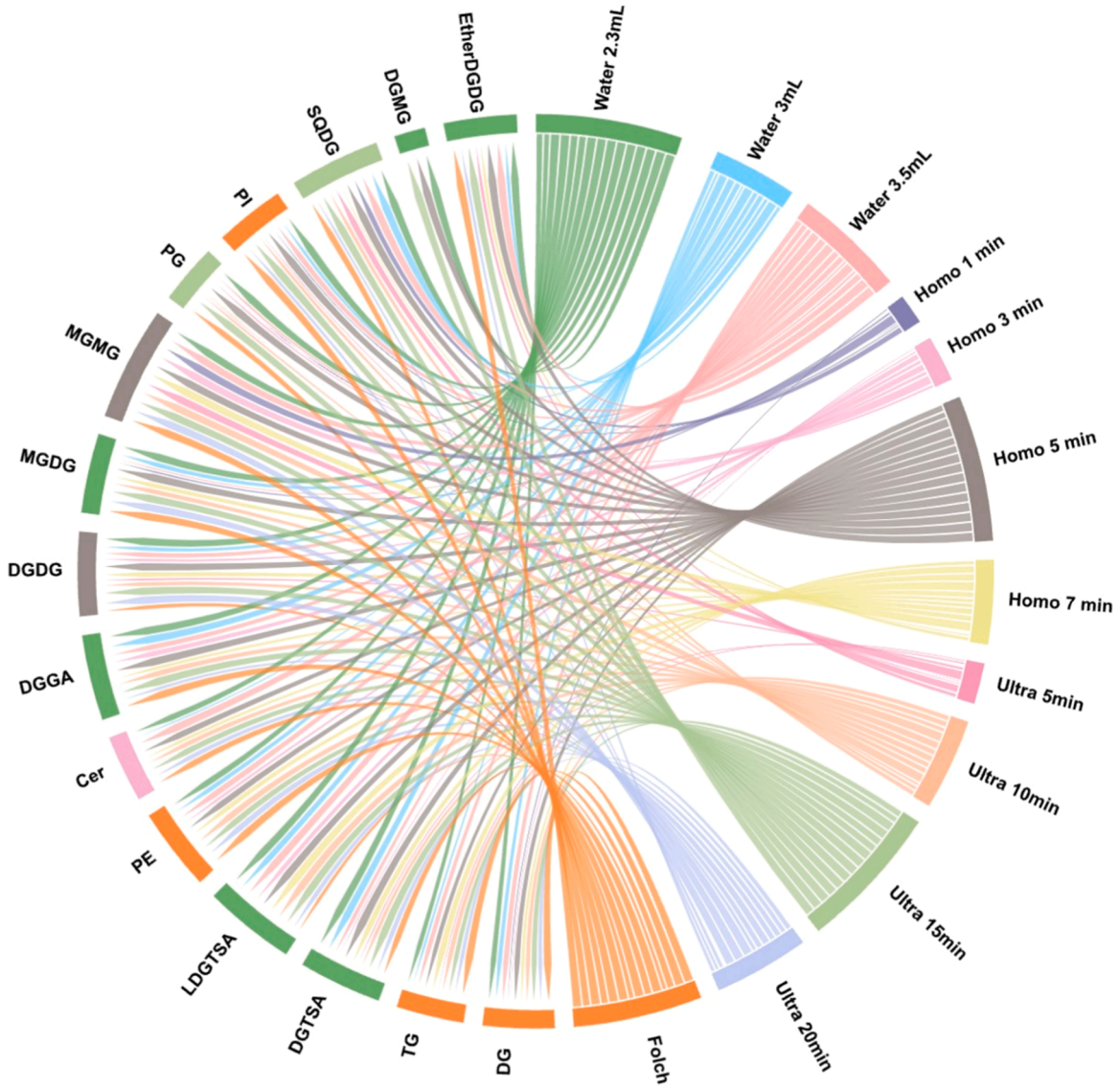

Fig. 6. Chord diagram depicting the number of lipid classes within each class recovered by different extraction methods, where matching colours between a lipid class and an extraction method/treatment indicate the positive impact on the extraction of the specific lipid. Lipid classes: LDGTSA, lyso-DGTSA; DGTSA, diacylglyceryl-N,N,N-trimethylhomoserine/β-alanine; PE, phosphatidylethanolamine; LPE, lyso-PE; PI, phosphatidylinositol; PG, phosphatidylglycerol; MGDG, monogalactosyldiacylglycerol; DGDG, digalactosyldiacylglycerol; SQDG, sulfoquinovosyldiacylglycerol; EtherDGDG, ether-Linked digalactosyldiacylglycerol; Cer, ceramides; DGMG, digalactosylmonoglyceride; MGMG, monogalactosylmonoglyceride; DGGA, diacylglyceryl glucuronide; Cer, ceramide; TG, triglycerides; DG, diacylglycerol.

lipidomics data from different laboratories and studies comparable.

Studies in humans and animals

This study did not involve human or animal subjects.

CRediT authorship contribution statement

Cong Ding: Writing – original draft, Methodology, Formal analysis. **Mikael Fabritius:** Writing – review & editing, Methodology, Data curation. **Baoru Yang:** Writing – review & editing, Supervision, Funding acquisition, Conceptualization.

Declaration of competing interest

The authors declare the following financial interests/personal relationships which may be considered as potential competing interests:

Baoru Yang reports financial support and equipment, drugs, or supplies were provided by Research Council of Finland. Cong Ding reports financial support was provided by Finland-China Food and Health Network. Cong Ding reports financial support was provided by EDUFI Fellowship. Baoru Yang reports equipment, drugs, or supplies was provided by European Union-NextGenerationEU. If there are other authors, they declare that they have no known competing financial interests or personal relationships that could have appeared to influence the work reported in this paper.

Acknowledgement

Dr. Jari Hänninen at the Biodiversity Unit of the University of Turku is warmly thanked for providing the *F. vesiculosus* sample for the study. This study was funded by the Research Council of Finland (Decision No 356891, Structures and functions of chiral lipids: a stereospecific & multiomics approach). The personal grants for Cong Ding from the Finland-China Food and Health Network and the EDUFI Fellowship are acknowledged. The research was supported by European Union-

NextGenerationEU instrument funding for the national FOODNUTRI infrastructure network.

Supplementary materials

Supplementary material associated with this article can be found, in the online version, at doi:10.1016/j.afres.2026.101967.

Data availability

Data will be made available on request.

References

Bardou, P., Mariette, J., Escudié, F., Djemiel, C., & Klopp, C. (2014). jvenn: An interactive Venn diagram viewer. *BMC bioinformatics, 15*, 293. https://doi.org/10.1186/1471-2105-15-293

BLIGH, E. G., & DYER, W. J. (1959). A rapid method of total lipid extraction and purification. *Canadian journal of biochemistry and physiology, 37*, 911–917. https://doi.org/10.1139/o59-099

Bowden, G. D., Pichler, B. J., & Maurer, A. (2019). A design of experiments (DoE) approach accelerates the optimization of copper-mediated 18F-fluorination reactions of arylstannanes. *Scientific reports, 9*, Article 11370. https://doi.org/10.1038/s41598-019-47846-6

Cao, X., Xu, M., Feng, T., Li, R., Song, Y., Meng, N., Fan, X., Zeng, J., & Xu, J. (2024). A comparative lipid profile of four fish species: From muscle to industrial by-products based on RPLC−Q-TOF-MS/MS. *Food research international (Ottawa, Ontario), 191*, Article 114725. https://doi.org/10.1016/j.foodres.2024.114725

Carreira-Casais, A., Otero, P., Garcia-Perez, P., Garcia-Oliveira, P., Pereira, A. G., Carpena, M., … Prieto, M. A. (2021). Benefits and drawbacks of ultrasound-assisted extraction for the recovery of bioactive compounds from marine algae. *International Journal of Environmental Research and Public Health, 18*, 9153. https://doi.org/10.3390/ijerph18179153

Conde, T., Lopes, D., Pais, R., Batista, J., Maurício, T., Rey, F., Melo, T., Domingues, P., & Domingues, R. (2024). Discovering oxidized polar lipids in microalgae lipidome using liquid chromatography mass spectrometry approaches. *Algal research, 84*, Article 103764. https://doi.org/10.1016/j.algal.2024.103764

Coniglio, D., Bianco, M., Ventura, G., Calvano, C. D., Losito, I., & Cataldi, T. R. I. (2021). Lipidomics of the edible brown Alga Wakame (*Undaria pinnatifida*) by liquid chromatography coupled to electrospray ionization and tandem mass spectrometry. *Molecules (Basel, Switzerland), 26*, 4480. https://doi.org/10.3390/molecules26154480

Da Costa, E., Domingues, P., Melo, T., Coelho, E., Pereira, R., Calado, R., Abreu, M. H., & Domingues, M. R. (2019). Lipidomic signatures reveal seasonal shifts on the relative abundance of high-valued lipids from the brown algae *fucus vesiculosus*. *Marine Drugs, 17*, 335. https://doi.org/10.3390/md17060335

Du, N., Sun, Y., Chen, Z., Huang, X., Li, C., Gao, L., Bai, S., Wang, P., & Hao, Q. (2023). Effects of multiple freeze-thaw cycles on protein and lipid oxidation, microstructure and quality characteristics of rainbow trout (*Oncorhynchus mykiss*). *Fishes, 8*, 108. https://doi.org/10.3390/fishes8020108

Figueiredo, A. R. P., Da Costa, E., Silva, J., Domingues, M. R., & Domingues, P. (2019). The effects of different extraction methods of lipids from *Nannochloropsis oceanica* on the contents of omega-3 fatty acids. *Algal research, 41*, Article 101556. https://doi.org/10.1016/j.algal.2019.101556

Ganguly, M., Debraj, D., Mazumder, N., Carpenter, J., Manickam, S., & Pandit, A. B. (2024). Impact of ultrasonication on the oxidative stability of oil-in-water nanoemulsions: Investigations into kinetics and strategies to control lipid oxidation. *Industrial & engineering chemistry research, 63*, 10212–10225. https://doi.org/10.1021/acs.iecr.4c00506

Gao, X., Luo, J., Lü, L., Zhang, L., Zhang, S., & Cui, J. (2018). RNA-seq and UHPLC-Q-TOF/MS based lipidomics study in *Lysiphlebia japonica*. *Scientific reports, 8*, 7802. https://doi.org/10.1038/s41598-018-26139-4

Gowda, S. G. B., Yifan, C., Gowda, D., Tsuboi, Y., Chiba, H., & Hui, S.-P. (2022). Analysis of antioxidant lipids in five species of dietary seaweeds by liquid chromatography/mass spectrometry. *Antioxidants, 11*, 1538. https://doi.org/10.3390/antiox11081538

Han, X., & Gross, R. W. (2022). The foundations and development of lipidomics. *Journal of lipid research, 63*, Article 100164. https://doi.org/10.1016/j.jlr.2021.100164

Heavisides, E., Rouger, C., Reichel, A. F., Ulrich, C., Wenzel-Storjohann, A., Sebens, S., & Tasdemir, D. (2018). Seasonal variations in the metabolome and bioactivity profile of *fucus vesiculosus* extracted by an optimised, pressurised liquid extraction protocol. *Marine Drugs, 16*, 503. https://doi.org/10.3390/md16120503

Hoffmann, D. Y., & Shachar-Hill, Y. (2023). Do betaine lipids replace phosphatidylcholine as fatty acid editing hubs in microalgae? *Frontiers in plant science, 14*, Article 1077347. https://doi.org/10.3389/fpls.2023.1077347

Ishibashi, Y., Nagamatsu, Y., Miyamoto, T., Matsunaga, N., Okino, N., Yamaguchi, K., & Ito, M. (2014). A novel ether-linked phytol-containing digalactosylglycerolipid in the marine green alga, *Ulva pertusa*. *Biochemical and biophysical research communications, 452*, 873–880. https://doi.org/10.1016/j.bbrc.2014.08.056

Iverson, S. J., Lang, S. L. C., & Cooper, M. H. (2001). Comparison of the bligh and dyer and folch methods for total lipid determination in a broad range of marine tissue. *Lipids, 36*, 1283–1287. https://doi.org/10.1007/s11745-001-0843-0

Karageorgou, D., Rova, U., Christakopoulos, P., Katapodis, P., Matsakas, L., & Patel, A. (2023). Benefits of supplementation with microbial omega-3 fatty acids on human health and the current market scenario for fish-free omega-3 fatty acid. *Trends in Food Science & Technology, 136*, 169–180. https://doi.org/10.1016/j.tifs.2023.04.018

Kind, T., Liu, K.-H., Lee, D. Y., DeFelice, B., Meissen, J. K., & Fiehn, O. (2013). LipidBlast in silico tandem mass spectrometry database for lipid identification. *Nature methods, 10*, 755–758. https://doi.org/10.1038/nmeth.2551

Kobayashi, K. (2016). Role of membrane glycerolipids in photosynthesis, thylakoid biogenesis and chloroplast development. *Journal of plant research, 129*, 565–580. https://doi.org/10.1007/s10265-016-0827-y

Kumari, P., Reddy, C. R. K., & Jha, B. (2011). Comparative evaluation and selection of a method for lipid and fatty acid extraction from macroalgae. *Analytical biochemistry, 415*, 134–144. https://doi.org/10.1016/j.ab.2011.04.010

Lam, S. M., Tian, H., & Shui, G. (2017). Lipidomics, en route to accurate quantitation. *Biochimica et biophysica acta. Molecular and cell biology of lipids, 1862*, 752–761. https://doi.org/10.1016/j.bbalip.2017.02.008

Li, Q., Zhao, Y., Zhu, D., Pang, X., Liu, Y., Frew, R., & Chen, G. (2017). Lipidomics profiling of goat milk, soymilk and bovine milk by UPLC-Q-Exactive Orbitrap mass spectrometry. *Food chemistry, 224*, 302–309. https://doi.org/10.1016/j.foodchem.2016.12.083

Lopes, D., Rey, F., Leal, M. C., Lillebø, A. I., Calado, R., & Domingues, M. R. (2021). Bioactivities of lipid extracts and complex lipids from seaweeds: Current knowledge and future prospects. *Marine Drugs, 19*, 686. https://doi.org/10.3390/md19120686

Marques, F., Lopes, D., Conde, T., Melo, T., Silva, J., Abreu, M. H., Domingues, P., & Domingues, M. R. (2023). Lipidomic characterization and antioxidant activity of macro- and microalgae blend. *Life (Chicago, Illinois : 1978), 13*, 231. https://doi.org/10.3390/life13010231

Montone, C. M., Cavaliere, C., Cerrato, A., Laganà, A., Piovesana, S., Taglioni, E., & Capriotti, A. L. (2024). Detailed lipid investigation of edible seaweeds by photochemical derivatization and untargeted lipidomics. *Analytical and bioanalytical chemistry, 416*, 6269–6282. https://doi.org/10.1007/s00216-024-05573-6

Pham, T. H., Thomas, R., Schwab, C., Martinez, M. M., & Vidal, N. P. (2024). Unraveling the neutral and polar lipidome of Nordic brown macroalgae: A sustainable source of functional lipids. *Food Chemistry, 459*, Article 140415. https://doi.org/10.1016/j.foodchem.2024.140415

Rakusanova, S., & Cajka, T. (2024). Tips and tricks for LC–MS-based metabolomics and lipidomics analysis. *TrAC Trends in Analytical Chemistry, 180*, Article 117940. https://doi.org/10.1016/j.trac.2024.117940

Rey, F., Lopes, D., Maciel, E., Monteiro, J., Skjermo, J., Funderud, J., Raposo, D., Domingues, P., Calado, R., & Domingues, M. R. (2019). Polar lipid profile of saccharina latissima, a functional food from the sea. *Algal Research, 39*, Article 101473. https://doi.org/10.1016/j.algal.2019.101473

Saini, R. K., Prasad, P., Shang, X., & Keum, Y.-S. (2021a). Advances in lipid extraction methods—A review. *International journal of molecular sciences, 22*, Article 13643. https://doi.org/10.3390/ijms222413643

Shimojima, M. (2011). Biosynthesis and functions of the plant sulfolipid. *Progress In Lipid Research, 50*, 234–239. https://doi.org/10.1016/j.plipres.2011.02.003

Smedes, F., & Askland, T. K. (1999). Revisiting the development of the bligh and Dyer total lipid determination method. *Marine Pollution Bulletin, 38*, 193–201. https://doi.org/10.1016/S0025-326X(98)00170-2

Sun, T., Wang, X., Cong, P., Xu, J., & Xue, C. (2020). Mass spectrometry-based lipidomics in food science and nutritional health: A comprehensive review. *Comprehensive reviews in food science and food safety, 19*, 2530–2558. https://doi.org/10.1111/1541-4337.12603

Suzuki, H., Cuiné, S., Légeret, B., Wijffels, R. H., Hulatt, C. J., Li-Beisson, Y., & Kiron, V. (2025). Phosphorus starvation induces the synthesis of novel lipid class diacylglyceryl glucuronide and diacylglyceryl- *N,N,N* -trimethylhomoserine in two species of cold-adapted microalgae *Raphidonema* (Chlorophyta). *The Plant journal : for cell and molecular biology, 121*, Article e17227. https://doi.org/10.1111/tpj.17227

Tsugawa, H., Ikeda, K., Takahashi, M., Satoh, A., Mori, Y., Uchino, H., Okahashi, N., Yamada, Y., Tada, I., Bonini, P., Higashi, Y., Okazaki, Y., Zhou, Z., Zhu, Z.-J., Koelmel, J., Cajka, T., Fiehn, O., Saito, K., Arita, Masanori, & Arita, Makoto (2020). A lipidome atlas in MS-DIAL 4. *Nature Biotechnology, 38*, 1159–1163. https://doi.org/10.1038/s41587-020-0531-2

Uhoraningoga, A., Kinsella, G. K., Henehan, G. T., & Ryan, B. J. (2018). The Goldilocks approach: A review of employing design of experiments in prokaryotic recombinant protein production. *Bioengineering, 5*, 89. https://doi.org/10.3390/bioengineering5040089

Ulmer, C. Z., Jones, C. M., Yost, R. A., Garrett, T. J., & Bowden, J. A. (2018). Optimization of Folch, Bligh-Dyer, and Matyash sample-to-extraction solvent ratios for human plasma-based lipidomics studies. *Analytica Chimica Acta, 1037*, 351–357. https://doi.org/10.1016/j.aca.2018.08.004

Wang, H., Yang, L., Wang, X., Cong, P., Xu, J., & Xue, C. (2022). Comprehensive lipidomic analysis of three edible brown seaweeds based on reversed-phase liquid chromatography coupled with quadrupole time-of-flight mass spectrometry. *Journal Of Agricultural And Food Chemistry, 70*, 4138–4151. https://doi.org/10.1021/acs.jafc.1c07513